Sensors & Transducers

On-Chip Integrated Silicon Photonic Thermometers

[1, 2] **Nikolai N. KLIMOV,** [3] **Thomas PURDY,** [1] **Zeeshan AHMED**

[1] Thermodynamic Metrology Group, Sensor Science Division, Physical Measurement Laboratory,
National Institute of Standards and Technology, Gaithersburg, MD 20899, USA
[2] Joint Quantum Institute, University of Maryland, College Park, MD 20742, USA
[3] Quantum Optics Group, Quantum Measurement Division, Physical Measurement Laboratory,
National Institute of Standards and Technology, Gaithersburg, MD 20899, USA

Abstract: The fundamental limitations of resistance-based thermometry and the desire to reduce sensor ownership cost have produced considerable interest in the development of photonics-based temperature sensors as an alternative to resistance thermometers. Photonic temperature sensors have the potential to leverage advances in frequency metrology to provide cost effective measurement solutions. We report on the fabrication and characterization of photonic-based nanoscale thermometers. Two types of temperature sensors, described in this work, a silicon photonic Bragg grating cavity and photonic crystal cavity devices, were fabricated using silicon-on-insulator CMOS-technology. The devices have built-in Fabry-Perot cavities, resonance's wavelength of which shifts systematically with temperature. The sensitivity of photonic nanoscale thermometers can be tuned by a top-cladding material. When cladded with a poly (methyl methacrylate) thin layer, the sensitivity is ≈ 70 pm/°C, on the other hand, cladding with a silicon dioxide layer gives an improved sensitivity of ≈ 80 pm/°C. The described photonic thermometers have a temperature sensitivity that is at least seven to eight times better, compared to the sensitivity of conventional fiber Bragg grating sensors. We demonstrate that silicon photonic nanoscale thermometers are a viable temperature sensing solution. *Copyright © 2015 IFSA Publishing, S. L.*

Keywords: Photonic thermometer, Photonic crystal cavity, Waveguide Bragg grating.

1. Introduction

Though today's resistance thermometers can routinely measure temperatures with uncertainties of 10 mK, they are sensitive to environmental variables such mechanical shock and humidity, which cause the sensor resistance to drift over time requiring expensive, time consuming calibrations [1]. These fundamental limitations of resistance thermometry, as well as the desire to reduce sensor ownership cost has produced considerable interest in the development of photonic temperature sensors as an alternative to resistance thermometers. The list of proposed alternative solutions ranges macroscale functionalized dyes [2], hydrogels [3], fiber Bragg grating sensors [2, 4, 5], and microscale silicon photonic devices [6–9]. In this study we present our results on fabrication and characterization of our first generation silicon photonic thermometers: a silicon waveguide Bragg grating cavity (Si WBGC) and silicon photonic crystal cavity (Si PhCC) sensors.

Previously [10] we demonstrated the performance of Si WBGC and Si PhCC thermometers cladded with a poly (methyl methacrylate) (PMMA)[1] layer. In this work we expand our recent results [11] on

---

[1] Disclaimer: Certain commercial fabrication facility, equipment, materials or computational software are identified in this paper in order to specify device fabrication, the experimental procedure and data analysis adequately. Such identification is not intended to imply endorsement by the National Institute of Standards and Technology, nor is it intended to imply that the facility, equipment, material or software identified are necessarily the best available.

investigation the sensors' performance, when they are cladded with a silicon dioxide (SiO_2) layer. Both types of SiO_2 – cladded photonic thermometers, Si WBGC and Si PhCC, over the range from 20 °C to 120 °C show a systematic upshift of the resonance wavelength of ≈ 82 pm/°C as temperature increases. For comparison, when cladded with PMMA, the sensors show the sensitivity of only ≈ 70 pm/°C [10]. An increased sensitivity due to SiO_2 – cladding is at least a factor of eight better compared to conventional FBG-based thermometers [2, 4, 5].

2. Results and Discussion

2.1. Device Fabrication, Measurement Setup

The operating principle of silicon photonics-based temperature sensors is based on temperature dependence of silicon's refractive index, which is determined by a high thermo-optic coefficient of silicon [12]. The temperature-driven variations of silicon refractive index induce a nearly linear shift of the photonic device's transmission and/or reflection spectra towards longer (or shorter) wavelengths, when the sensor is being heated (or cooled). On the other hand, a temperature-induced wavelength shift, and thus the temperature itself, can be measured very precisely using recent advances in frequency metrology.

The temperature sensors described in this work are silicon photonic devices that have a built-in Fabry-Perot (F-P) cavity, with resonance peak corresponding to the telecom frequency range (from ≈ 1300 nm to ≈ 1700 nm). The photonic devices were fabricated at the National Institute of Standards and Technology (NIST), the Center of Nanoscale Science and Technology (CNST), using silicon-on-insulator (SOI) CMOS-technology via electron beam lithography followed by a selective inductive coupled plasma reactive ion etch (ICP RIE) of 220 nm-thick topmost silicon layer of the SOI wafer. After ICP RIE etch the devices were top-cladded with 700 nm-thick PMMA or 800 nm-thick SiO_2 protective layer.

The photonic thermometers are characterized using a custom built measurement setup (Fig. 1).
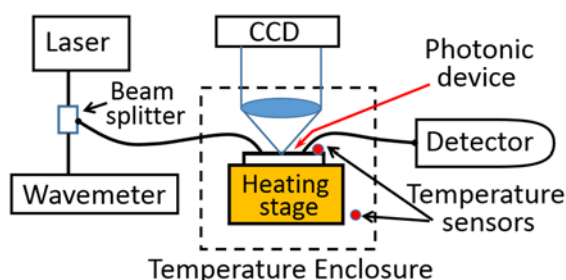

Fig. 1. Schematic diagram of the measurement setup for characterizing photonics-based thermometers.

In this setup a C-band laser (New Focus TLB-6700 series) is swept over the sensor resonance. Ten percent of laser power was immediately picked up from the laser output for wavelength monitoring (HighFinesse WS/7) while the rest, after passing through the photonic device, was detected by a large sensing-area power meter (Newport, model 1936-R). Light was coupled into and out of the waveguide using on-surface focusing grating couplers [13].

### 2.2. Performance of Photonic Temperature Sensors

The first type of thermometers, Si WBGC, is based on a silicon nanowaveguide with a cross-section of 510 nm × 220 nm that sits on top of 3 μm-thick buried oxide layer (BOX) of the SOI substrate (Fig. 2a). The central part of the sensor is a 327 nm-long F-P cavity surrounded on its opposite sides by two Bragg mirrors, which are made via a periodic modulation of the silicon nanowaveguide's effective refractive index. The refractive index modulation is achieved by changing the width of the nanowaveguide in a periodic square-wave form with 60 nm modulation amplitude and a period of 330 nm.
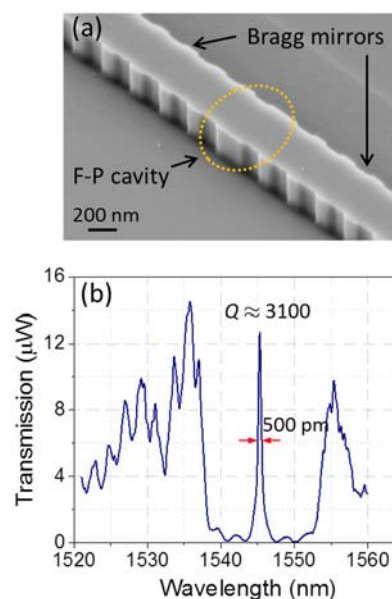
Fig. 2. (a) SEM image of Si WBGC thermometer before top-cladding. (b) Transmission spectrum of SiO_2 – cladded Si WBGC thermometer measured at 20 °C.

The characteristic transmission spectrum of Si WBGC, cladded with 800 nm-thick layer of SiO_2, is shown on Fig. 2b. It features a roughly 14 nm-wide stopband centered around 1546 nm at 20°C and an F-P cavity resonance peak (with a peak width of FWHM ≈ 500 pm and a quality factor of $Q \approx 3100$) located at the stopband's center. The stopband's width and center, as well as FWHM of the resonance peak are mainly determined by the Bragg grating mirrors' design parameters. As we changed the

temperature from 20 °C to 120 °C the whole transmission spectrum of Si WBGC, including the sharp F-P cavity resonance peak, shifts linearly towards higher wavelengths (Fig. 3a) at a rate of $\delta\lambda/\delta T \approx 82$ pm/°C (Fig. 3b).
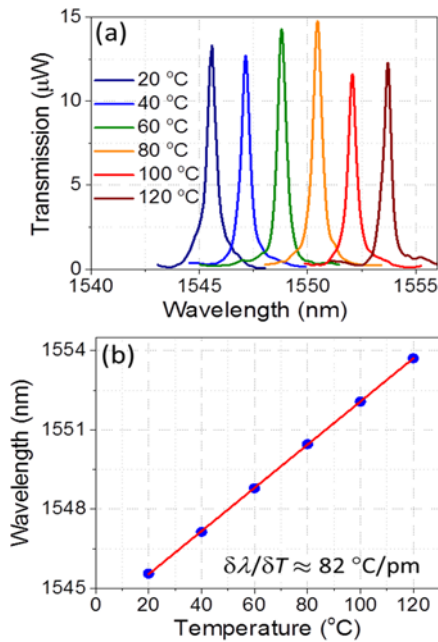

Fig. 3. (a) Transmission spectra of resonance peak of SiO₂ – cladded Si WBGC thermometer measured at different temperatures: color curves from left to right correspond to $T = (20, 40, 60, 80,$ and $100)$ °C, respectively. (b) Temperature dependence of the resonance peak's position.

The second type of thermometers, a silicon photonic crystal cavity (Si PhCC) shown on Fig. 4a is similar to Si WBGC. This is also an F-P cavity-type photonic device operating around the telecom frequency range. The Si PhCC consists of an 800 nm-wide silicon nanowaveguide and an F-P cavity located at the sensor's center. Two Bragg mirrors located on the opposite sides of the F-P cavity are one-dimensional photonic crystals, consisting of a pattern of subwavelength holes in a silicon nanowaveguide with diameters that vary gradually from 170 nm to 200 nm. Our design follows the deterministic approach of Refs. [14-15], in which the Si PhCC features a zero-length F-P cavity and two adjacent photonic crystal modulated Bragg mirrors with a Gaussian field attenuation that maximizes the Q of the cavity. For Si PhCC sensor shown on Fig. 4a the light is coupled into the F-P cavity via an evanescent coupling from a 510 nm-wide bus-nanowaveguide placed within ≈ 300 nm from the Si PhCC active area. As for Si WBGC sensors, Si PhCC devices were cladded with 800 nm of a silicon dioxide layer.

Fig. 4b shows a transmission spectrum of SiO₂ – cladded Si PhCC sensor measured at 20 °C. It features three resonance peaks, marked A, B and

C, which correspond to the fundamental, the first and the second F-P cavity modes, respectively.
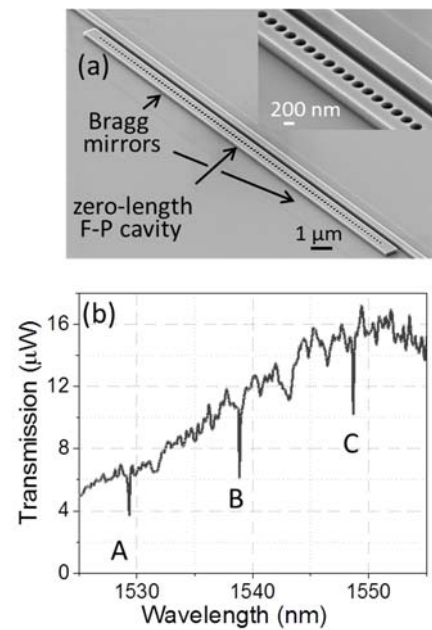
Fig. 4. (a) SEM image of Si PhCC thermometer before the top-cladding. (b) Transmission spectrum of SiO₂ – cladded Si PhCC thermometer measured at 20 °C. Fundamental, 1st, and 2nd modes are marked by A, B and C, respectively.

The peaks are much narrower compared to the resonance peak of Si WBGC: for the 1st mode the peak width is ≈ 60 pm and $Q \approx 26000$ (Fig. 5a). As temperature is varied the whole spectrum shifts. Shown on Fig. 5a are the spectra of the 1st mode resonance peak measured at temperatures ranging from 20 °C to 120 °C. The corresponding thermal sensitivity of the Si PhCC is ≈ 83 pm/°C (Fig. 5b), similar to the sensitivity of the Si WBGC device.

Photonic sensors described above where top-cladded with a silicon dioxide layer. We also investigated the performance of devices cladded with a PMMA layer. Fig. 6 shows a Si PhCC sensor and its temperature sensitivity performance, when it is top-cladded with a 700 nm-thick PMMA layer. The design of this sensor is similar to the one shown on Fig. 4a, except that the light is coupled not evanesently, but directly through a feeding nanowaveguide. The inset on Fig. 6b shows a fundamental mode resonace peak measured at different temperatures between 20°C and 40°C. Although this device is of a higher quality factor ($Q \approx 30600$) compared to the previously described sensors, it sensitivity is reduced ($\delta\lambda/\delta T \approx 68$ pm/°C) due to a negative thermo-optic coefficient of PMMA [10, 16–18].

Although a PMMA-cladding can be done very fast via a spin-coating, the working temperature range is limited by PMMA's glass transition temperature (≈ 85°C) [10].
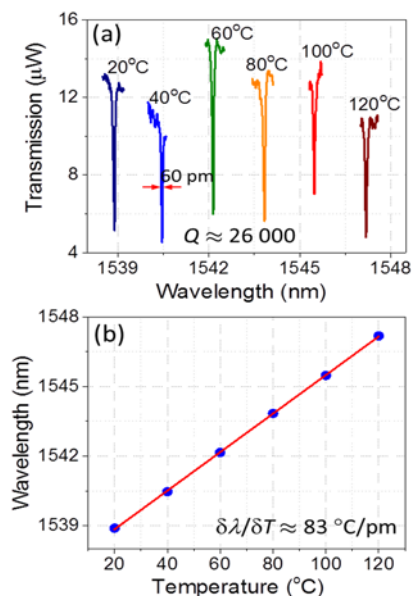
Fig. 5. (a) Transmission spectra of the resonance peak of SiO$_2$ – cladded Si PhCC corresponding to the first mode of the F-P cavity measured at different temperatures from 20°C to 120°C. (b) Temperature dependence of the first mode F-P cavity resonance peak's position.
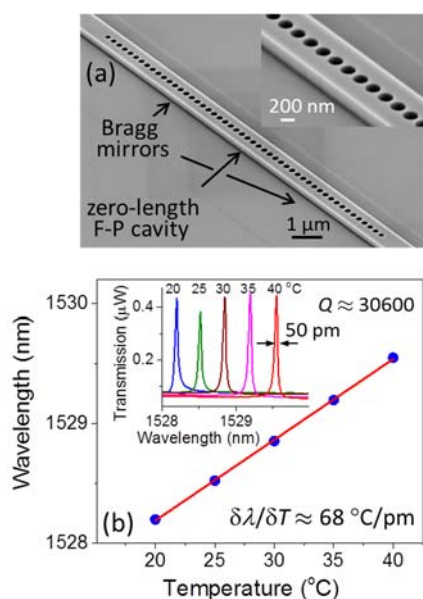
Fig. 6. (a) SEM image of Si PhCC thermometer before top-cladding. Inset zooms in the central part of the sensor. (b) Temperature dependence of the wavelength position of the resonance peak corresponding to the fundamental mode of the F-P cavity of the PMMA-cladded Si PhCC sensor. Inset shows the transmission spectra of the resonance peak corresponding to the fundamental mode measured at $T = (20, 25, 30, 35$ and $40)$°C.

3. Summary

In this work we present our results on the fabrication and characterization of two types of F-P cavity-based photonic nanothermometers, Si WBGC and Si PhCC. The thermal response of these sensors was measured in the temperature range

from 20 °C to 120 °C. Compared to a PMMA-cladding, the silicon dioxide cladding increases the thermometers' sensitivity ($\delta\lambda/\delta T$) from ≈ 68 pm/°C to ≈ 82 pm/°C. This represents at least a factor of eight improvement over the sensitivity of conventional fiber Bragg sensors [2, 4-5]. In addition, SiO$_2$ – cladding extends the allowed temperature range, when compared to PMMA-cladded photonic sensors, which upper allowed temperature (≈ 85 °C for PMMA used in Ref. [10]) is limited by PMMA's glass transition temperature. While both types of F-P cavity-based sensors, Si WBGC and Si PhCC, show a similar thermal sensitivity, the Si PhCC thermometer has several advantages. It not only has a smaller footprint, but also has a resonance peak, which is narrower by about a factor of 10. This in turn reduces the combined measurement uncertainty by a factor of ten. We expect that a careful design of the Si PhCC would give an even higher Q, further increasing the device's temperature resolution and improving measurement uncertainty. While our devices have similar temperature sensitivity as the previously reported ring resonator [6–9], unlike the ring resonator these sensors allow for unambiguous determination of the fundamental mode. The inability to unambiguously identify ring resonator modes limits the temperature measurement range to one free spectral range (typically $\Delta T \approx 50$ K to 170 K). Removing this ambiguity increases the temperature range of photonic temperature devices to potentially cover the temperature range from 4 K to 1300 K. In summary, we demonstrated that both types of silicon photonic thermometers can be a future replacement of resistance-based thermometers.

Acknowledgement

References

[1]. G. F. Strouse, Standard Platinum Resistance Thermometer Calibrations from the Ar TP to the Ag FP, *NIST Spec. Publ.*, 250, 81, 2008, pp. 84-85.

[2]. J. S. Donner, S. A. Thompson, M. P. Kreuzer, G. Baffou, R. Quidant, Mapping Intracellular Temperature Using Green Fluorescent Protein, *Nano Lett.*, 12, 4, 2012, pp. 2107-2111.

[3]. E. M. Ahmed, Hydrogel: Preparation, characterization, and applications: A review, *J. Adv. Res.*, 6, 2015, pp. 105–121.

[4]. S. J. Mihailov, Fiber Bragg Grating Sensors for Harsh Environments, *Sensors*, 12, 2012, pp. 1898–1918.

[5]. A. Kersey, T. A. Berkoff, Fiber-optic Bragg-grating differential-temperature sensor, *IEEE Photonics Technol. Lett.*, 4, 1992, pp. 1183-1185.

[6]. M.-S. Kwon, W. H. Steier, Microring-resonator-based sensor measuring both the concentration and

temperature of a solution, *Optics Express*, 16, 13, 2008, pp. 9372-9377.

[7]. B. Guha, K. Preston, M. Lipson, Athermal silicon microring electro-optic modulator, *Optics Letters*, 37, 12, 2012, pp. 2253-2255.

[8]. G.-D. Kim, H.-S. Lee, C.-H. Park, S.-S. Lee, B. T. Lim, H. K. Bae, *et al*., Silicon photonic temperature sensor employing a ring resonator manufactured using a standard CMOS process, *Optics Express*, 18, 2010, pp. 22215–22221.

[9]. H. Xu, M. Hafezi, J. Fan, J. M. Taylor, G. F. Strouse, Z. Ahmed, Ultra-sensitive chip-based photonic temperature sensor using ring resonator structures, *Optics Express*, 22, 3, 2014, pp. 3098-3104.

[10]. N. N. Klimov, T. Purdy, Z. Ahmed, Fabry-Perot cavity-based silicon photonic thermometers with ultra-small footprint and high sensitivity, in *Proceedings of the Conference Advanced Photonics Congress*, Boston MA, 2015, paper SeT4C.4.

[11]. N. N. Klimov, T. Purdy, Z. Ahmed, Fabrication and Characterization of On-Chip Integrated Silicon Photonic Bragg Grating and Photonic Crystal Cavity Thermometers, in *Proceedings of the Conference Nanotechnology*, Washington DC, 2015.

[12]. G. Cocorullo, F. G. D. Corte, I. Rendina, Temperature dependence of the thermo-optic coefficient in crystalline silicon between room temperature and 550 K at the wavelength of 1523 nm, *Applied Physics Letters*, 74, 1999, pp. 3338-3340.

[13]. F. Van Laere, G. Roelkens, M. Ayre, J. Schrauwen, D. Taillaert, D. Van Thourhout, *et al.*, Compact and Highly Efficient Grating Couplers Between Optical Fiber and Nanophotonic Waveguides, *J. Light. Technol.*, 25, 2007, pp. 151-156.

[14]. Q. Quan, P. B. Deotare, M. Loncar, Photonic crystal nanobeam cavity strongly coupled to the feeding waveguide, *Applied Physics Letters*, 96, 2010, pp. 203102-203102.

[15]. Q. Quan, M. Loncar, Deterministic design of wavelength scale, ultra-high Q photonic crystal nanobeam cavities, *Optics Express*, 19, 19, 2011, pp. 18529-18542.

[16]. T. Watanabe, N. Ooba, Y. Hida, M. Hikita, Influence of humidity on refractive index of polymers for optical waveguide and its temperature dependence, *Applied Physics Letters*, 72, 13, 1998, pp. 1533-1535.

[17]. S. T. Chu, W. Pan, S. Suzuki, B. E. Little, S. Sato, Y. Kokubun, Temperature insensitive vertically coupled microring resonator add/drop filters by means of a polymer overlay, *IEEE Photonics Technology Letters*, 11, 1999, pp. 1138-1140.

[18]. L. Xiang, C. Zhuang-Qi, S. Qi-Shun, Y. Yan-Fang, Study on the thermo-optic properties of DR1/PMMA composite, *Chinese Physics*, 15, 10, 2006, pp. 2439-2444.

───────────────────